Mesoscopic theory of shear banding and crack propagation in metallic glasses

G. P. Zheng[1] and M. Li[2,*]
[1]*Department of Mechanical Engineering, The Hong Kong Polytechnic University, Hung Hom, Kowloon, Hong Kong, China*
[2]*School of Materials Science and Engineering, Georgia Institute of Technology, Atlanta, Georgia 30332, USA*
(Received 18 June 2009; published 23 September 2009)

We propose a phenomenological theory to model shear banding, shear-band propagation and branching on mesoscopic scales in metallic glasses by using Ginzburg-Landau formulism. The disordering caused by mechanical or thermal agitation is represented by atomic volume dilatation and used as an order parameter. This model captures several important features in the deformation process, namely, shear localization or banding, shear-band propagation and branching, and crack propagation and its velocity. We also assessed the relation between the crack propagation velocity and local heating and the connection between the serrated flow and shear band branching.

DOI: 10.1103/PhysRevB.80.104201 PACS number(s): 62.25.Mn, 46.50.+a, 61.43.Bn, 61.43.Fs

One of the most promising developments in metallic materials in recent years is the invention of bulk metallic glasses (BMGs).[1,2] BMGs are topologically disordered solids without the long-range translational order as seen in crystalline materials. The disordered structure with atoms packed randomly leads to many unique and outstanding properties. Perhaps the most interesting is the phenomenon called shear localization: when a metallic glass subject to external load reaches the flow stress, plastic deformation occurs in narrow bands. The deformation strain inside the band is many times larger than that outside, causing samples to fail locally and quickly. The shear localization is by far identified as the only mechanism that affects the strength, ductility, and thus application of the BMGs which otherwise have many potential applications derived from the superb properties.[1–4] Shear banding consists of three stages: *nucleation*, *growth and propagation*, and *final failure*; and each stage occurs on a different spatial and temporal scale. Shear-band nucleation occurs in less than microsecond and with the critical nucleation size of about 10 to several hundred nanometers, depending on the material and ambient conditions.[1–5] Once the critical state is approached, the band could grow and propagate; the bands grow into steady state, or maturity with typical thickness of tens of nanometers to hundreds of nanometers and length of many times larger than the thickness, depending on the propagation condition.[1–5] A propagating shear band often becomes unstable, resulting in branching into subbands.[1–5] The mechanical properties of metallic glasses are determined by the detailed behavior of the shear-band evolution. For example, a shear band starting propagating would affect yielding, or strength, and its propagation and branching would contribute to ductility as more deformation is concentrated inside the bands, absorbing more deformation energy and thus contributing to higher toughness. In addition, as we identify below, shear-band branching may be a major reason for the serrated flow observed during plastic deformation.

The evolution exhibited in a localized shear band is a complex interplay of many factors. The initiation of a shear band is related to the local stress concentration and increase of the number of displaced atoms during deformation via *atomic volume dilatation* (AVD).[6,7] As shown by extensive molecular-dynamics (MD) simulation recently,[8,9] the volumetric change is necessary for atomic displacement in the environment that has no obvious plastic-strain-carrier defects such as dislocations as in crystals. Such mechanism was first hypothesized by Erying[10] for viscous flow in liquids and later by Spaepen in deformation of metallic glasses.[6,7] Furthermore, the growth and propagation of a shear band is a result of not only atomic volume dilatation, but also local stress state, temperature, and other structural entities such as inclusions, voids, and chemical heterogeneities.[1–5,11] Despite encouraging progresses made so far, our understanding of shear-banding process in terms of quantitative description and modeling of various shear-banding phenomena observed in experiments are still very limited, largely due to the vast span of the length and time scales in the processes. For instance, the shear bands, especially those in the propagation state, are either too large for MD simulation to simulate their branching and interaction processes,[8,9] or too small for the finite element method (FEM) to capture its atomistic scale deformation details.[12,13] In this paper, we develop a phenomenological theory on mesoscopic scale to bridge this gap and use phase-field approach to simulate shear-band formation and propagation in metallic glasses.

As mentioned above, the basic premise of the theory is that plastic deformation is carried by the microscopic flow defects, AVD. As proposed by Eyring,[10] the deforming atoms swapping positions with the dilated open space nearby enable the flow or plastic deformation. Such an open space was called *free volume* as its size was thought to be comparable to a hole about the size of an atom,[7,14] thus costing nearly no energy for the atom-hole swapping. However, we shall not follow this definition here as we have known from the atomistic simulations that it is not necessary to have such a large hole, or free volume, for the system to execute plastic flow.[8,9,15] For this reason, we simply use the dilatation of atomic volume defined by $v_f = v_i - v_0$, where v_i is the atomic volume defined as, for instance, the volume of the Voronoi polyhedron of the ith atom, v_0 is the molar volume in the undeformed ideal random close packing (RCP) state. The detailed description of the quantities and their rendition on atomic scale can be found in Refs. 8 and 9. In the theory, we shall use the fraction or density of AVD as an order parameter represented by a coarse-grained scalar phase field at position $\vec{r}$ as $\rho(\vec{r}) = v_f/(v_m - v_0)$, where v_m is the maximum dilated volume when complete decohesion occurs at that position, which corresponds to a reasonable estimate of v_m of

a few atomic spacing. We should mention in passing that the reference state defined above does not affect the results for deformation as long as we can define such a state consistently. Based on the nature of AVD defects and the characteristics of plastic deformation of glassy alloy, clearly, the order parameter defined this way is not conserved while the mass is, which is very different from the deformation in crystalline materials where volumetric change is negligible. The dilatation can be thermally or mechanically activated. As shown in both experiment[1–5] and atomistic simulations,[8,9] at temperature well below the glass transition temperature T_g and under the applied stress $\sigma \ll \sigma_f$, where σ_f is the flow stress, the amorphous solid acts like an elastic medium with few sites with large AVD activated. As σ approaches σ_f, the AVD sites can be activated by applied stress,[7,15] or by local heating[3,16] due to excessive plastic deformation. When the accumulation of these activated AVD sites reaches a critical value, shear bands are observed to form.[6,7,17] Further growth of the AVD defects could lead to fracture.

Based on these phenomenological accounts for the deformation and fracture characteristics of metallic glasses from atomic scales, known also experimentally on continuum level, we could write the free-energy density of the system as a function of the AVD through a Ginzburg-Landau formulism as[18]

$$f_\rho = \frac{a}{2}\rho^2 + \frac{b}{3}\rho^3 + \frac{c}{4}\rho^4 + \cdots, \tag{1}$$

where a, b, and c are the Landau coefficients depending on temperature, strain, chemical composition, or other state variables. We should make a note that the use of a single scalar quantity ρ as a "state variable" to describe the deformation process in metallic glasses is tantamount to assuming that it encapsulates the changes from other quantities such as local atomic packing, chemical composition, and short- and medium-range topological order, and so on. In fact, the atomistic simulation did provide some direct support for this assumption.[8,9] Incidentally, one could include these quantities explicitly in a statistical physics model such as ours. But it would be much complicated, if not impossible, to monitor the evolution of the state of the system in a simple and transparent way, especially in the disordered systems such as metallic glasses. For these considerations, we shall use the AVD, a scalar quantity for the time being. Specifically, the selection of the expression of Eq. (1) is based on the following reasoning: (1) when $\rho(\vec{r}) \to 0$, $f_\rho = 0$, where the system remains in an undeformed, ideal RCP state. (2) The presence of certain degree of disorder from the reference state gives rise to the increase in free energy at the state represented by $\rho(\vec{r}) \neq 0$. The cubic term indicates such a state while a negative value for $\rho(\vec{r})$ is not realistic. Therefore, each different $\rho(\vec{r})$ represents a state in the free-energy landscape, which naturally includes an infinite number of these states with different $\rho(\vec{r})$ in the metastable glassy system under deformation. (3) Fracture occurs when $\rho(\vec{r}) \to 1$.

In addition, in a deforming continuum media, there is also the strain energy associated with long-range elastic field originated from the external applied load and the defects, i.e., AVD, produced during deformation process. We can write the strain energy of an isotropic medium as

$$e[\varepsilon] = \frac{1}{2} C_{ijkl} \varepsilon_{kl} \varepsilon_{ij}, \tag{2}$$

where ε_{ij} is the strain tensor defined by the displacement field $\mathbf{u}$ through the relation $\varepsilon_{ij} = (\partial u_j / \partial x_i + \partial u_i / \partial x_j)/2$ with $i,j = 1,2,3$; $C_{ijkl} = \mu(\delta_{ik}\delta_{jl} + \delta_{il}\delta_{jk}) + \lambda \delta_{ik}\delta_{jl}$ is the elastic constants; μ is the shear modulus and λ is Lamé coefficient related to the bulk modulus B by $B = \lambda + 2\mu/3$. Therefore, for a metallic glass subject to external loading, the total free-energy density can be written as

$$f(\rho, \varepsilon_{ij}) = e[\varepsilon_{ij}] + f_\rho = e[\varepsilon_{ij}] + \frac{a}{2}\rho^2 + \frac{b}{3}\rho^3 + \frac{c}{4}\rho^4 + O(\rho^5). \tag{3}$$

Equation (3) is a general expression for the free energy contributed from the primary order parameter, ρ, and a secondary order parameter ε_{ij}. As we mentioned, physically we would expect to see the interaction between the two as the AVD is influenced by deformation, and vise versa. Since the free energy $f(\rho, \varepsilon_{ij})$ on the left-hand side of Eq. (3) is a scalar, we can only allow the interaction energy, to the few lower order terms in terms of ρ and ε_{ij}. Such approach, as done routinely in Landau theory, can be recovered by using a perturbation scheme as shown in the following: Because the magnitude of AVD is usually very small [0.1–1.0 % (Refs. 8, 9, and 15)] in the elastic region ($\sigma < \sigma_f$), we can expand the coefficients of Eq. (1) in terms of $\Delta e = e[\varepsilon_{ij}] - e_0$ at $\sigma \sim \sigma_f$ when the sample is undergoing *plastic deformation*,

$$\begin{aligned} a &= a_0 + a_1 \Delta e + a_2 (\Delta e)^2 + \cdots, \\ b &= b_0 + b_1 \Delta e + b_2 (\Delta e)^2 + \cdots, \\ c &= c_0 + c_1 \Delta e + c_2 (\Delta e)^2 + \ldots, \end{aligned} \tag{4}$$

where e_0 is the strain energy at the elastic limit. a_0, b_0 and c_0 are independent of the strain. Since for most metallic glasses, the increment of the strain at the onset of plastic flow is limited, the expansion in terms of the plastic work Δe is justified, thus providing a coupling between AVD and strain. Assuming the leading error term of $\Delta e \cdot \rho^4$ or $(\Delta e)^2 \cdot \rho^2$ in Eq. (1), the local free-energy density of a metallic glass can thus be approximated as[19]

$$f(\rho, \varepsilon_{ij}) = e[\varepsilon_{ij}] + \frac{a_0}{2}\rho^2 + \frac{b_0}{3}\rho^3 + \frac{c_0}{4}\rho^4 + \left(\frac{a_1}{2}\rho^2 + \frac{b_1}{3}\rho^3\right)(e[\varepsilon_{ij}] - e_0). \tag{5}$$

The coefficients a_0, b_0, and c_0 of Eq. (5) depend on other external state variables. Therefore, Eq. (5) describes the energy landscape of a metallic glass containing AVD defects when subject to deformation. The advantage of the above approach is that we may take into account some of the plastic strains at the onset of flow in the Landau theory which otherwise would be limited to the elastic regime [Eq. (3)]. Since the dependence of AVD is explicitly specified in the above formulation, we describe the temperature dependence of the AVDs by assuming a linear relation between a_0 and tempera-

ture T, $a_0=a'-b'\frac{T}{T_g}$, where a' and b' are constants.

To describe the evolution of the AVDs and thus shear band which is nothing but a spatial variation of deformation in the sample described by two variables, ρ and ε_{ij}, we also include the kinetic energy, $K=\frac{\rho_0}{2}[\dot{\vec{u}}]^2$ and the gradient term of the AVD in the free energy,

$$F=\int\left\{\frac{\rho_0}{2}[\dot{\vec{u}}]^2+f(\rho,\varepsilon_{ij})+\frac{\kappa}{2}|\vec{\nabla}\rho|^2\right\}dV, \tag{6}$$

where ρ_0 is the mass density of the sample. The second term in the integral is described in Eq. (5) and the third term is the gradient energy of the AVDs where κ represents the "interfacial" energy between the regions with different amount of deformation or AVD. When a crack appears, it becomes the surface energy, which is depicted by the Griffith model.[19]

From the standard protocols of the Ginzburg-Landau formulism, the equations of motions for $\vec{u}$ and ρ are described respectively by

$$\tau_\rho\frac{\partial\rho}{\partial t}=-\frac{\delta F}{\delta\rho}=\kappa\nabla^2\rho-(a_0\rho+b_0\rho^2+c_0\rho^3)-\rho(a_1+b_1\rho)\times(e[\varepsilon_{ij}]-e_0) \tag{7a}$$

and

$$\rho_0\frac{\partial^2\vec{u}}{\partial t^2}=-\nabla\cdot\left[\frac{\delta F}{\delta\varepsilon_{ij}}\right]=\mu\nabla\cdot\left\{\left[1+\rho^2\left(\frac{a_1}{2}+\frac{b_1}{3}\rho\right)\right]\nabla\vec{u}\right\}, \tag{7b}$$

where τ_ρ is the characteristic time for AVD activation. Equations (2) and (7) govern the local strains and the evolution of AVDs generated by both the plastic and the plastic deformation in metallic glasses respectively and thus form a complete set of equations describing the dynamics of deformation and fracture. It is worth to point out that an effective shear elastic modulus obtained in Eq. (7b) for a locally homogeneous system, is dependent of the amount of AVD, which is inline with the observation of the softening of the elastic modulus caused by deformation found in atomistic simulation[17] as well as experiment.[1–5] Moreover, the local heating due to the localized plastic strain can be described by the heat conduction equation,

$$k\nabla^2T+\beta\frac{\partial Q}{\partial t}=C_P\rho_0\frac{\partial T}{\partial t}, \tag{7c}$$

where $Q=\int\sigma_{ij}d\varepsilon_{ij}$ is the total mechanical work and β is the coefficient representing the percentage of the conversion of mechanical work into heat, or Taylor-Quinney coefficient. $\beta=1$ represents the adiabatic heating whereas $\beta=0$ is the isothermal process. k is the thermal conductivity and C_P is the heat capacity. By solving Eq. (7), the shear banding resulting from the evolution of mechanical deformation and AVDs can be readily obtained.

In the following, we shall present a simple case study using this theory for shear-band propagation, branching, and cracking, as we know that neither atomistic simulation nor continuum modeling could treat this case satisfactorily.[8,9,12,13] The reason to choose this case first is based on the following considerations: First, as known shear bands are often generated from cracks[1–5] and second, it is relatively easy numerically to implement the theory and generate localized deformation from a crack. More case studies with different scenarios and loading modes will be presented elsewhere. We consider a model glass made of Vitrelloy 1 ($Zr_{41}Ti_{14}Ni_{10}Cu_{12.5}Be_{22.5}$) under a mode I cracking since the experimental measurement of various properties for this system is the most complete and available. As shown in Fig. 1(a), the system used has dimensions of $20\times20\times2$ μm^3, and a rectangular crack with dimensions of 0.4×0.05 μm^2. The materials properties are listed as follows:[20,21] $T_g=625$ K, the Young's modulus $E=95$ GPa, Poisson's ratio $\nu=0.35$, $\rho_0=6050$ kg/m^3, $k=5$ (W/m)K^{-1}, $C_P=475$ (J/kg)K^{-1}. The elastic strain limit under uniaxial tension is $\varepsilon_f\sim2\%$. The characteristic time of AVD activation is $\tau_\rho=0.25$ ns.[22] The coefficients of Eq. (7) are given by $a_0=4(2-T/T_g)\Delta G$, $b_0=-32\Delta G$, and $c_0=16\Delta G$, where the AVD activation energy ΔG is estimated as 4.6 eV at $T=300$ K.[23] We choose $a_1=4$ and $b_1=-9$ to quantitatively describe the shear softening in glassy alloy, which is consistent with experiments and MD simulation.[17,21] In particular, such chosen coefficients reflect the fact that the shear modulus tends to decrease and approaches zero when $\rho(\vec{r})\to1$. We define that a shear band forms in a region where $\rho>\rho_c=0.8$ (Ref. 24) and cracking or fracture occurs if $\rho\to1$. The parameter κ in Eq. (7) cannot be directly obtained from experiment but could be estimated from the surface energy γ by $\kappa=\gamma R$, where $R=0.56$ μm is the characteristic length of the vein pattern at the fracture surface of Zr-based BMG observed in experiments. We have calculated γ for $Zr_{41}Ti_{14}Ni_{10}Cu_{12.5}Be_{22.5}$ using density-functional theory[25] and found $\gamma\sim1.97$ J/m^2.[26]

We solve the partial differential equations numerically in the model system shown in Fig. 1(a). The length rescale factor $l_r=\sqrt{\kappa/\mu e_0}$ and time rescale factor $t_0=l_r/\sqrt{\mu/\rho_0}$ are used to reduce Eq. (7) to dimensionless equations. Hence l_r and t_0 represent the characteristic length and the time scale of the system respectively. We use triangle meshes for the model system. The sizes of meshes can be as small as 2 nm near the regions of initial crack. These features are essential in the numerical simulation since Eq. (7) are typical stiff equations because of the shear localization. We made sure that the size is large enough so the simulation results are not dependent on it. Figure 1(b) shows the stress states near the shear band.

We first focus on shear-band initiation and propagation from the crack by neglecting the local heating ($\beta=0$). Shear band starts from the initial crack and grows into a propagating crack when the stress intensity factor $K=\sigma\sqrt{l\pi}$ is larger than 21.03 Mpa(m)$^{1/2}$, which has been successfully captured by our phase-filed modeling as shown in Figs. 1(c)–1(e). We can see that the shear band accumulated with activated AVDs is highly localized in a 50-nm-thick region. As shown in Figs. 1(c)–1(e), when the applied tensile stress increases, the shear band could change from a straight line to a wavy curve and finally become unstable. The instability of the shear-band propagation results in branching of the shear band. The fracture toughness obtained from the simulation is $K_{IC}=22.1$ Mpa(m)$^{1/2}$ at which the crack starts to propagate,

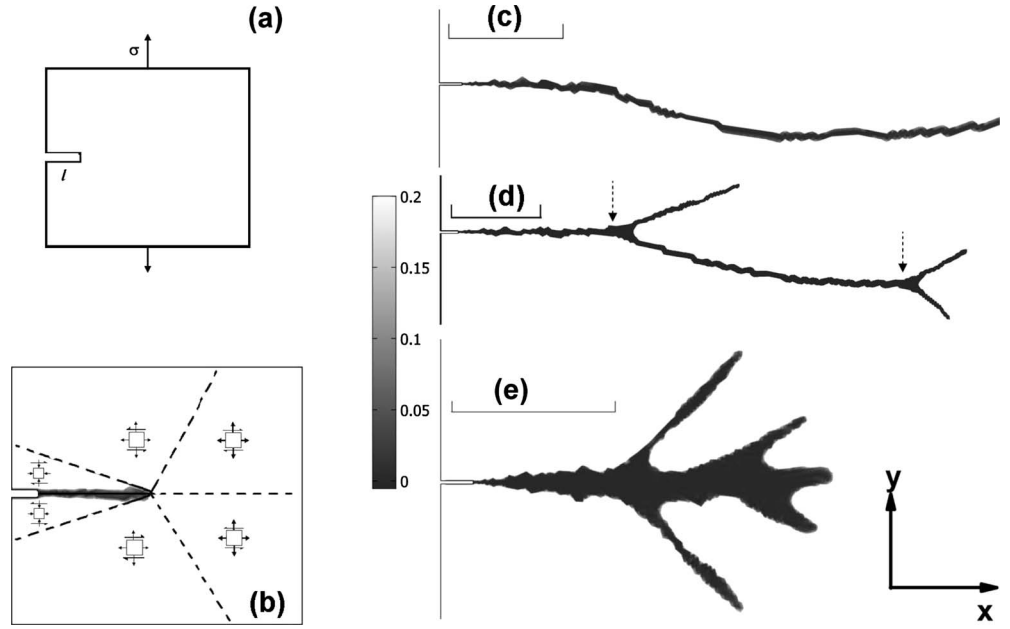

FIG. 1. (a) The model system of a BMG plate ($20\times20\times2$ μm^3). A uniaxial tensile stress is applied along the y direction. $l=0.4$ μm is the length of initial crack. (b) Indications of stresses (σ_{xx}, σ_{yy} and σ_{xy}) around a single shear band. Both the magnitudes and directions of the stresses are shown. (c)–(e) Shear bands and crack propagations under stress intensity factors $K=25$, 35.4, and 100.2 MPam$^{1/2}$ respectively. Only a strip of the BMG plate is shown. The gray scales correspond to the values of $1-\rho$. The length bar represents 2 μm.

which is consistent with experiments. In addition, under large applied load, multiband branching [Fig. 1(e)] occurs in a way similar to that observed in experiments.[27]

Next we focus on the velocity of a propagating crack, as we observed that branching has a large effect on propagation. We found that crack propagation velocity cannot excess a critical velocity V_C, which is an indication of shear-band branching. From the simulation we see that in the sample without local heating during deformation, the shear-band branching always occurs when the crack propagation velocity reaches $V_C=0.63V_R$, where V_R is the Rayleigh wave speed. Here we define the critical velocity V_C as the maximum propagation velocity of a crack tip. Shear-band branching always occurs after the velocity of crack tip reaches V_C. Figure 1(d) shows the shear-band branching and the arrows indicate the positions where the crack velocities are V_C.

It has been long debated[27] that local heating is another important characteristic cause associated with shear banding, but at what stage and in what form heating is relevant to shear banding remains unclear. Because of the rapid advance of shear-band front and small spatial scale of a shear band,[28] temperature rise near the shear-band is difficult to measure from experiments.[29] We now can use the phase-field model to check how temperature rise affects shear-band propagation by considering the conduction of heat generated from plastic work [Eq. (7c)]. Figure 2 shows the temperature rise near the shear band at different values of β for the sample under the same loading condition. We can observe not only the dramatic temperature rise if β is close to 1, but also that the temperature rise near a shear band significantly affects the critical velocity V_C and the shear-band branching: Shear band can easily become unstable and branching occurs since V_C drops with increasing shear-band temperature. Such phenomenon is quantitatively characterized here. Figure 3 shows the velocity $V(t)$ of crack tip and the temperature at the crack tip under different applied loading stresses in the sample with $\beta=1$. Again we observe that V_C is a critical velocity for shear-band branching since the crack will slow down and finally stop after the shear-band branching occurs. It is found that V_C is insensitive to the applied stress then, so is the maximum temperature T_R at the crack tip. Interestingly, the maximum temperature T_R always occurs after the crack propagation velocity reaches V_C, suggesting the mechanism in that the local heating plays a less important role in the shear-band branching. When β increases from 0 to 1, the temperature rise $\Delta T=T_R$-300 (K) changes from 0 K to more than 2700 K if all the plastic work is converted into heat. The relation is determined as

$$\Delta T \sim \beta^x, \tag{8}$$

where $x=0.54$ as shown in Fig. 4. By measuring the V_C associated ΔT under different ratios β, the relation between V_C and temperature rise is shown in Fig. 4, which follows the scaling relation,

$$0.63V_R - V_C \propto (\Delta T)^y, \tag{9}$$

where $y=1.1$. The scaling relation indicates that the maximum velocity that a crack can achieve in Zr-based BMG is $0.63V_R$. However, in reality, the actual temperature rise depends on sample size, dimension, and ambient temperature, and importantly on crack opening which also conducts heat. So the crack propagation velocity should be well below $0.63V_R$ in most BMGs. Incidentally, the branching that occurs intermittently could cause the serrated flow observed widely in metallic glasses. Current understanding of the ser-

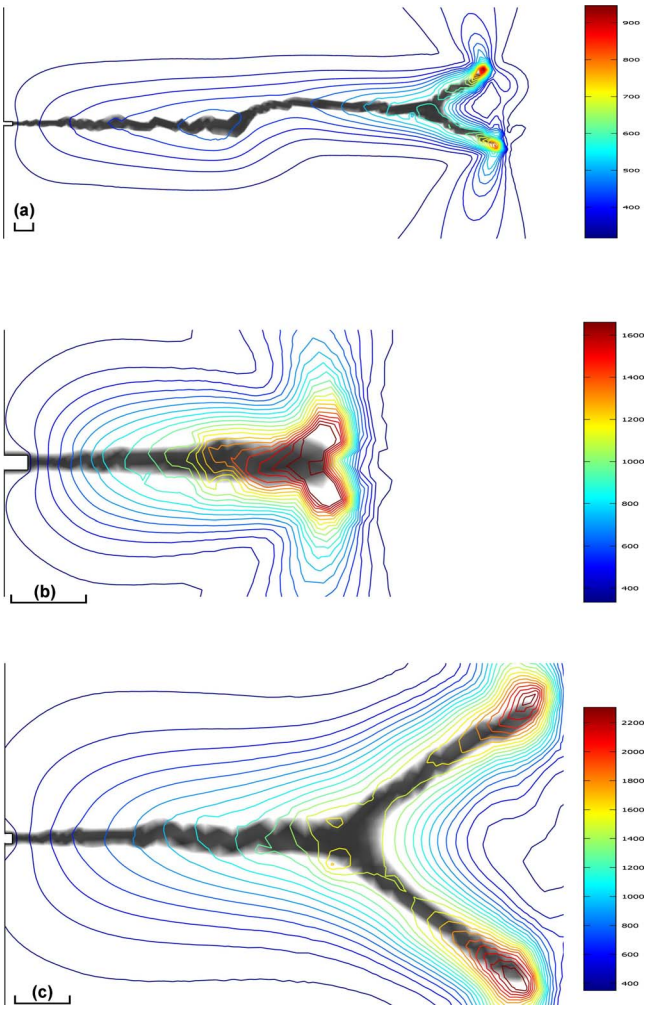

FIG. 2. (Color online) Temperature distribution around the shear band in the BMG with various plastic work to heat conversion ratios β and stress intensity factors K. (a) $\beta=0.1$. $K=27.7$ MPam$^{1/2}$. (b) $\beta=0.5$. $K=24.3$ MPam$^{1/2}$. (c) $\beta=1$. $K=20.1$ MPam$^{1/2}$. The color bars are for the contour plots of temperatures. Shear bands are shown in gray with the same scale as that in Fig. 1.

rated flow is centered mainly on generation of new shear bands.[1–5,30] Large efforts have been made to correlate each shear band formation with a serration observed in the force-displacement curve (or stress-strain relation). Our results offer a more convincing explanation to the phenomenon. Branching or shear band instability during propagation makes a considerable contribution to the serrated flow since nucleating a new shear band is much more costly energetically when there is already a propagating shear band.

In summary, based on the available results from both atomistic simulation and experiment, a Ginzburg-Landau formulism is developed to describe deformation in metallic glasses, in particular shear localization. The basis of this theory is that (1) the atomic volume dilatation is a primary internal state variable that describes the state of deformation and reflects the change of local topological and chemical order and thermal mechanical property change, (2) the deformation in metallic glass is governed by the evolution of the

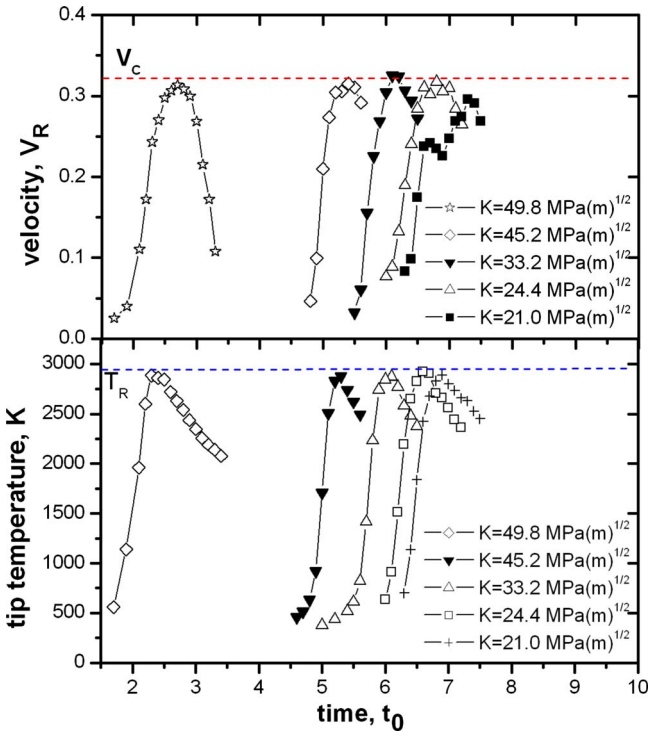

FIG. 3. (Color online) Crack propagation velocity and temperature rise of a shear band in the Zr-based BMG plate with a plastic work to heat conversion ratios $\beta=1$. Upper: The time-dependent velocity $V(t)$ of crack tip after it propagates from the initial crack. The time t in unit of t_0 is measured with respected to the moment when a uniaxial tensile stress σ is applied. $V(t)$ under various stress intensity factors K are shown. Lower: The corresponding time-dependent temperatures at the shear-band tip under various K.

free energy consisting of the contributions from the internal variable, the atomic volume dilatation, the strain energy of the sample under deformation, and the interaction between

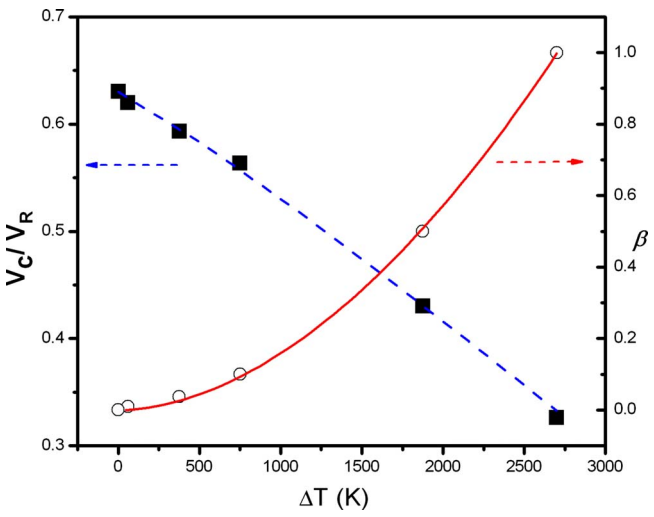

FIG. 4. (Color online) The relation between V_C and ΔT (solid symbols) and the relation between ΔT and β (open symbols) in Zr-based metallic glass plates with various plastic work to heat conversion ratios β. The blue dash line is the fit using Eq. (9). The red solid line is the fit for $\Delta T \sim \beta^x$ using Eq. (8).

the two, and (3) the infinite large number of the metastable states known to the glassy materials can be described in the free-energy landscape, $f(\rho, \varepsilon_{ij})$. Coupled with thermal transport, the dynamic equations [Eqs. (7)] governing ρ and ε_{ij} form a complete set of relations that determine the evolution of deformation and shear localization in metallic glasses. We should mention that the theory is different from the approach developed by Eyring and Spaepen earlier and later spearheaded by Langer *et al.* in that a transition state theory is used to describe the evolution of the damages incurred in amorphous solids with the energetics governing the transition probability supplemented separately.[6,7,10,31] We took Zr-based BMGs as an example and show that the phase-field model proposed can indeed reproduce some of the salient features in the deformation processes that otherwise are difficult to capture with atomistic and continuum modeling: (a) the formation of shear bands is observed with thickness about 50 nm prior to fracture, (b) the branching of shear bands occurs during plastic deformation, and (c) the temperature elevation due to local heating, which can affect the shear-band branching instability significantly. We also found that the serrated flow observed often in metallic glasses may be closely related to the shear-band instability, i.e. branching and propagation intermittency. This model provides a bridge for our understanding of the mechanical behaviors of BMG at mescoscopic scales, which is expected to lead to better prediction of shear-band behavior and lay a solid foundation for design and development of strong and ductile BMGs.

The authors are grateful for the financial supports provided initially for this work by DOE (Grant No. DEFG02-99ER45784) and the Johns Hopkins University, and currently by ARO (Grant No. ARO-W911NF-07-01-0490), NSF (Grant No. NSF-0907320) and a grant from the Research Grants Council of the Hong Kong Special Administrative Region, China (Project No. PolyU 7196/06E).

*Corresponding author; mo.li@mail.gatech.edu

[1] W. L. Johnson, JOM **54**, 40 (2002).
[2] A. Inoue and A. Takeuchi, Mater. Sci. Eng., A **375**, 16 (2004).
[3] C. A. Pampillo, J. Mater. Sci. **10**, 1194 (1975).
[4] H. Chen, Rep. Prog. Phys. **43**, 353 (1980).
[5] Z. F. Zhang, F. F. Wu, W. Gao, J. Tan, Z. G. Wang, M. Stoica, J. Das, J. Eckert, B. L. Shen, and A. Inoue, Appl. Phys. Lett. **89**, 251917 (2006).
[6] A. S. Argon, Acta Metall. **27**, 47 (1979).
[7] F. Spaepen, Acta Metall. **25**, 407 (1977).
[8] Q. K. Li and M. Li, Appl. Phys. Lett. **88**, 241903 (2006).
[9] Q. K. Li and M. Li, Mater. Trans. **48**, 1816 (2007).
[10] H. Eyring, J. Chem. Phys. **4**, 283 (1936).
[11] J. Eckert, J. Das, S. Pauly, and S. Duhamel, J. Mater. Res. **22**, 285 (2007).
[12] M. Zhao and M. Li, Appl. Phys. Lett. **93**, 241906 (2008).
[13] L. Anand and C. Su, J. Mech. Phys. Solids **53**, 1362 (2005).
[14] D. Turnbull and M. H. Cohen, J. Chem. Phys. **34**, 120 (1961).
[15] M. K. Flores, D. Suh, R. H. Dauskardt, P. Asoka-Kumar, P. A. Sterne, and R. H. Howell, J. Mater. Res. **17**, 1153 (2002).
[16] H. Chen, Y. He, G. J. Shiflet, and S. J. Poon, Nature (London) **367**, 541 (1994).
[17] Q. K. Li and M. Li, Phys. Rev. B **75**, 094101 (2007).
[18] G. P. Zheng, Ph.D. thesis, The Johns Hopkins University, 2001.
[19] See other formulations of phase-field model for cracking: L. O. Eastgate, J. P. Sethna, M. Rauscher, T. Cretegny, C.-S. Chen, and C. R. Myers, Phys. Rev. E **65**, 036117 (2002); A. Karma, D. A. Kessler, and H. Levine, Phys. Rev. Lett. **87**, 045501 (2001).
[20] R. D. Conner, A. J. Rosakis, W. L. Johnson, and D. M. Owen, Scr. Mater. **37**, 1373 (1997).
[21] H. A. Bruck, T. Christman, A. J. Rosakis, and W. L. Johnson, Scr. Mater. **30**, 429 (1994).
[22] S. V. Khonik, A. V. Granato, D. M. Joncich, A. Pompe, and V. A. Khonik, Phys. Rev. Lett. **100**, 065501 (2008).
[23] J. Lu, G. Ravichandran, and W. L. Johnson, Acta Mater. **51**, 3429 (2003).
[24] $\rho > 0.5$ when yielding occurs. We pick $\rho_c = 0.8$ to trace the band evolution graphically.
[25] G. Kresse and J. Furthmüller, Phys. Rev. B **54**, 11169 (1996).
[26] *Ab initio* simulation is performed in $Zr_{41}Ti_{14}Ni_{10}Cu_{12.5}Be_{22.5}$ glassy system consisting of 200 atoms using Vienna *ab initio* simulation package.
[27] P. Lowhaphandu and J. J. Lewandowski, Scr. Mater. **38**, 1811 (1998).
[28] K. M. Flores and R. H. Dauskardt, J. Mater. Res. **14**, 638 (1999).
[29] J. J. Lewandowski and A. L. Greer, Nature Mater. **5**, 15 (2006).
[30] R. Vaidyanathan, M. Dao, G. Ravichandran, and S. Suresh, Acta Mater. **49**, 3781 (2001).
[31] For example, M. L. Manning, J. S. Langer, and J. M. Carlson, Phys. Rev. E **76**, 056106 (2007), and references therein.